Nat. Hazards Earth Syst. Sci. Discuss., 1, 721–745, 2013
www.nat-hazards-earth-syst-sci-discuss.net/1/721/2013/
doi:10.5194/nhessd-1-721-2013

Natural Hazards
and Earth System
Sciences
Discussions
Open Access

A statistical feature of anomalous seismic activities prior to large shallow earthquakes in Japan revealed by the Pattern Informatics method

M. Kawamura[1], **Y.-H. Wu**[2], **T. Kudo**[3], **and C. C. Chen**[1]

[1]Department of Earth Sciences and Graduate Institute of Geophysics,
National Central University, Jhongli, Taoyuan 32001, Taiwan
[2]Department of Geology, University of California, Davis, CA 95616-8605, USA
[3]General Education Division, College of Engineering, Chubu University, Kasugai,
Aichi 487-0027, Japan

Received: 7 February 2013 – Accepted: 8 March 2013 – Published: 26 March 2013

Correspondence to: M. Kawamura (mkawamu@ncu.edu.tw)

Published by Copernicus Publications on behalf of the European Geosciences Union.

Abstract

For revealing the preparatory processes of large inland earthquakes, we systematically applied the Pattern Informatics method (PI method) to the earthquake data of Japan. We focused on 12 large earthquakes with magnitudes larger than $M = 6.4$ (an official magnitude of the Japan Meteorological Agency) that occurred at depths shallower than 30 km between 2000 and 2010. We examined the relation between the spatiotemporal locations of such large shallow earthquakes and those of PI hotspots, which correspond to the grid cells of anomalous seismic activities in a designated time span. Based on a statistical test using Molchan's error diagram, we inquired into the existence of precursory anomalous seismic activities of the large earthquakes and, if any, their characteristic time span. The test indicated that the Japanese $M \geqq 6.4$ inland earthquakes tend to be preceded by anomalous seismic activities of 8-to-10-yr time scales.

1 Introduction

Japan has been struck by many large inland earthquakes (e.g. the 2000 Western Tottori Prefecture Earthquake, the 2004 Mid Niigata Prefecture Earthquake, the 2005 West Off Fukuoka Prefecture Earthquake, the 2007 Noto Hanto Earthquake, the 2007 Niigataken Chuetsu-oki Earthquake, and the 2008 Iwate-Miyagi Nairiku Earthquake). Most of them occurred on faults that had not been considered active before their occurrences (Imanishi et al., 2006). Therefore, more detailed surveys on unknown active faults are required for modeling the occurrence mechanisms of large inland earthquakes and for calculating strong motions on various sites. Together with such studies, it is also important to examine the features of large inland earthquakes from statistical viewpoints. For comprehensively understanding the preparatory processes of large earthquakes, it is an important approach to systematically investigate the statistical features of seismic activities prior to large earthquakes.

Seismic activity is sensitive to stress in the crust (Dieterich, 1994; Dieterich et al., 2000; Toda et al., 2002). Therefore, investigation of temporal change in seismic activity is a key to understanding of the temporal variation in stress, which may in turn leads to obtaining information on the possibility of the occurrence of a future large earthquake. Temporal changes in seismic activities before large earthquakes have been reported for various regions including Alaska (Bufe et al., 1994; Kisslinger and Kindel, 1994), California (Bowman et al., 1998; Bowman and King, 2001; Bufe and Varnes, 1993; Jaume and Sykes, 1999; Papazachos et al., 2005; Resenberg and Matthews, 1988; Sobolev, 2003; Stuart, 1991; Sykes and Jaume, 1990), Central Asia (India/Eurasia collision zone) (Zheng et al., 1994), China (Wei, 1978; Yu et al., 2013), Greece (Karakaisis et al., 2002; Papazachos et al., 2005), Italy (Console et al., 2000), Japan (Huang et al., 2001; Mogi, 1969; Nagao et al., 2011; Ogata, 2004, 2005; Resenberg and Matthews, 1988; Papazachos et al., 2010; Katsumata, 2011a,b), Russia (Borovik, 1971), Taiwan (Chen, 2003; Chen et al., 2005, 2006; Chen and Wu, 2006; Wu and Chiao, 2006; Wu and Chen, 2007; Wu et al., 2008a,b, 2011), and Turkey (Öztürk and Bayrak, 2012).

These previous studies imply that anomalous seismic activities are associated with the preparatory processes of large earthquakes near their epicenters and in surrounding regions over various time scales. There are however few studies in which temporal changes in seismic activities prior to large earthquakes and their statistical characteristics that have systematically been investigated. For comprehensively understanding the preparatory processes of large earthquakes, systematic examination of precursory seismic activities is necessary. With the motivation, we systematically investigated precursory changes in seismic activities of large shallow earthquakes in Japan using Pattern Informatics (PI) method, which has retrospectively succeeded in identifying anomalous seismic activities prior to large earthquakes (Chen et al., 2005, 2006; Holliday et al., 2005, 2006; Rundle et al., 2002, 2003; Tiampo et al., 2002; Wu et al., 2008a,b, 2011). In data and methodology section, we introduce our analysis procedure to obtain a spatiotemporal PI map using the PI method, which identifies PI hotspots showing anomalous change in seismic activity. The spatiotemporal PI map illustrating the relations between the spatiotemporal locations of anomalous seismicity areas and those of shallow large earthquakes, and Molchan's error diagrams are shown in results section and discussed in discussion and conclusions section.

2 Data and methodology

We used the earthquake catalog maintained by the Japan Meteorological Agency (JMA). JMA started a new operation of data processing in October 1997 by unifying earthquake catalogs maintained by different organizations. Furthermore, it started relocating past events using different velocity models and started changing the method for calculating JMA magnitude (M) in 2003. Accordingly, inhomogeneity in the earthquake catalog has been caused, which is mainly attributed to the variation of seismic networks, the improvements of observation instruments, and changes of data processing methods (Habermann, 1987; Nanjo et al., 2011; Resenberg and Matthews, 1988). Therefore, investigation of the spatial and temporal homogeneity of the JMA earthquake catalog is important for evaluating the temporal change in seismic activity. To examine the homogeneity of the catalog, we mapped minimum magnitude of completeness (M_c) with grid cell intervals of 60 km and 80 km at depths of 0 to 30 km since January 1980 using the method of Wiemer and Wyss (2000). In calculating M_c for each grid cell, its surrounding 200 earthquakes were used. Application of this method resulted in obtaining $M_c < 3.5$. This is also consistent with Fig. 2 of Huang et al. (2001) and Fig. 4 of Nanjo et al. (2010). Thus, we first used events with $M \geqq 3.5$ (cut-off magnitude of 3.5) in applying the PI method. Furthermore, in order to examine the effects of the use of different cut-off magnitudes on the statistical features of the spatiotemporal PI maps, we attempted the analyses using the events with $M \geqq 4.0$, and 4.5.

The PI method was originally developed based on the concept of pattern dynamics (Rundle et al., 2000). Stress can be regarded as a space-time state variable in a system of true deterministic dynamics, and is a fundamental measure that should be monitored for identifying its temporal change prior to a future large earthquake. Direct observation of stress change is, however, difficult because earthquakes occur below the surface of the earth. Hence, new instruments have been developed for observing seismic activity with higher precision and accuracy, which is considered to be a kind of stress sensor (Ma et al., 2005; Stein, 1999; Toda et al., 2000), based on seismographic information. We thus selected seismic activity as a space-time state variable of the pattern dynamics to investigate the change in an earthquake system.

The PI method was applied to the earthquake data in Japan (rectangular region in Fig. 1) as follows and shown in the flowchart of Fig. 2a.

1. Target region is set and divided into a designated interval of grid cells (60 km by 60 km for cut-off magnitude of 3.5 and 80 km by 80 km for that of 4.0 or 4.5).

2. Seismic intensity change $\Delta I_i(t_b, t_1, t_2)$ on i-th grid cell for a target time period (change interval) from t_1 to t_2 ($t_1 = t_2 - t_c (t_c = 4, 6, 8, 10, 12, \text{and } 14 \times 365$ days), $t_2 = 1$ October 1997–28 February 2011), is calculated to obtain the probability of earthquake occurrence in prediction period from t_2 to t_3. Seismic intensity $I_i(t_b, t)$ is defined as the number of earthquakes per day in a square area including i-th grid cell, which is averaged over the time period between a reference time t_b (t_0 (= 1 January 1980) $< t_b < t_1$) and t. A side of the square area is changed depending on cut-off magnitude: 204 km by 204 km for cut-off magnitude of 3.5 and 312 km by 312 km for that of 4.0 and 4.5. To obtain seismic intensity change, seismic intensities $I_i(t_b, t_1)$ and $I_i(t_b, t_2)$ for i-th grid cell for respective time period, i.e., t_b to t_1 and t_b to t_2, are calculated. Then, we calculate seismic intensity change $\Delta I_i(t_b, t_1, t_2) = I_i(t_b, t_2) - I_i(t_b, t_1)$.

3. Process (2) is repeated to obtain seismic intensity changes for all grid cells.

4. To extract the coherent trends in seismic intensity change during t_1 to t_2, seismic intensities $I_i(t_b, t_1)$ and $I_i(t_b, t_2)$ are calculated by shifting t_b from t_0 to t_1; then, seismic intensity change $\Delta I_i(t_b, t_1, t_2)$ is normalized temporally by subtracting its temporal mean and dividing by its temporal standard deviation. Furthermore,

$\Delta I_i(t_b, t_1, t_2)$ is also normalized spatially to highlight unusual seismic intensity changes. The value of $\Delta I_i(t_b, t_1, t_2)$ varies according to the grid cells where t_b is fixed; therefore, we can normalize it spatially by subtracting its spatial mean and then dividing by its spatial standard deviation for every value of t_b. The spatiotemporally normalized seismic intensity change is then obtained and denoted as $\Delta \hat{I}_i(t_b, t_1, t_2)$.

5. Most of the effects of random fluctuation in seismic intensity change and background seismic intensity change are eliminated by normalization. Accordingly, the preseismic change can be represented by the spatiotemporally normalized seismic intensity change $\Delta \hat{I}_i(t_b, t_1, t_2)$. Since the preseismic change during a preparatory process can be seismic quiescence, seismic activation, or even both, $\Delta \hat{I}_i(t_b, t_1, t_2)$ may be negative or positive. To incorporate all the preseismic change and reduce the fluctuation of random noise, we take the absolute value of spatiotemporally normalized seismic intensity $|\Delta \hat{I}_i(t_b, t_1, t_2)|$ and average the absolute value over all values of t_b to obtain $\langle|\Delta \hat{I}_i(t_b, t_1, t_2)|\rangle$.

6. Then, the probability of earthquake occurrence $P_i(t_1, t_2)$ is defined as $\langle|\Delta \hat{I}_i(t_b, t_1, t_2)|\rangle^2$ and the average probability as the mean μ_p of $P_i(t_1, t_2)$. Finally, the probability of earthquake occurrence relative to the background mean, $\Delta P_i(t_1, t_2) \equiv \langle|\Delta \hat{I}_i(t_b, t_1, t_2)|\rangle^2 - \mu_\mathrm{p}$, is further divided by the spatial maximum and is color coded and plotted as a PI hotspot.

7. The end of change interval t_2 is moved forward (t_1 and t_3 are accordingly changed by the same time interval) and processes (2) to (6) are conducted.

3 Results

Figures 3 to 5 shows the spatiotemporal PI maps for different cut-off magnitudes of 3.5, 4.0, and 4.5, in which grid cells with large changes in seismic activities (PI hotspots) for different lengths of change intervals (4, 6, 8, 10, 12, and 14 yr) are highlighted. Color grid cells with earthquake occurrence probabilities higher than −0.4 (toward zero) show the spatiotemporal locations with large changes in seismic activity, or seismic quiescence and activation. This indicates high probabilities of earthquake occurrences in prediction periods, the lengths of which equal to those of change intervals (Fig. 2). Red color grid corresponds to the largest change in seismic activity, which is regarded as highest probability of earthquake occurrence in prediction period. On the contrary, deep blue color grid lower than −0.4 show the location with small change in seismic activity, indicating low earthquake occurrence probability in prediction period. Red and white stars in each panel show the spatiotemporal locations of target ($M \geqq 6.4$) earthquakes (Table 1); red color ones indicate that target earthquakes occur in prediction periods following change intervals with earthquake occurrence probabilities higher than −0.4. Even if target events are included in grid cells with low earthquake occurrence probabilities in change intervals, as long as they are located next to grid cells with high earthquake occurrence probabilities in the same intervals, they are shown by using read color stars and are regarded as the events accompanied by anomalous seismic activities. On the contrary, white color ones indicate that they occur outside such prediction periods. For the sake of convenience, we hereinafter refer to the total spatiotemporal area occupied by prediction periods that follow change intervals with large seismicity changes (or high earthquake occurrence probabilities) as alarm area.

We here focus on whether each large earthquake occurs or not in alarm area. The numbers of red stars in Figs. 3 to 5 appear to be almost the same for all change intervals of 4, 6, 8, 10, 12, and 14 yr. It is, therefore, necessary to quantitatively compare the statistical performances of the spatiotemporal PI maps for different cut-off magnitudes and change intervals. For the purpose, we used Molchan's error diagram (Kagan, 2007; Molchan, 1997; Shcherbakov et al., 2010) to examine the coherence between the number of target ($M \geqq 6.4$) earthquakes located in/outside alarm area and fraction of grid cells occupied by alarm area. Figures 6 to 8 denote the plots of miss rate versus fraction of grid cells occupied by alarm area. Here, miss rate is defined as the number of $M \geqq 6.4$ events located outside alarm area, which is normalized by the total number of $M \geqq 6.4$ events. A line connecting (0,1) to (1,0) shows the random miss rate, which corresponds to no significant statistical performance. In calculating the lower 95 % confidence level of the random miss rate, we used the method of Zechar and Jordan (2008). In the statistical test, the variation of miss rate by that of alarm area is calculated by changing the lower threshold (−0.4) of high earthquake occurrence probabilities from the minimum to maximum for each diagram (open circles in Figs. 6 to 8). The best performance of the PI method is regarded to be in the bottom left corner (0,0). On the contrary, the performance on the upper-right side of the lower 95 % confidence level curve of the random miss rate is not regarded as statistically significant performance. It should therefore be focused on the rate of black open and solid circles that are located on the bottom-left side of the lower 95 % confidence level curve. The plot of miss rate versus fraction of grid cells occupied by alarm areas, which are denoted with black open circles and large black solid circles in Figs. 6 to 8, shows the largest rates of the circles located on the bottom-left side when 8- or 10-yr change intervals are adopted (panels c and d in Figs. 6 to 8). Therefore, the null hypothesis that there is no significant coherence between the locations of $M \geqq 6.4$ events and the number of grid cells occupied by alarm area was rejected at a confidence level of 95 % for those change intervals. This indicates that application of the PI method to the shallow earthquake data of Japan shows the best statistical performances when 8-to-10-yr change intervals are adopted. At the same time, the significant statistical performance implies that 8-to-10-yr change intervals reflect the characteristic time period of preparation for the occurrence of a large shallow earthquake in Japan.

4 Discussion and conclusions

We applied the PI method to the earthquake catalog of inland Japan. Since seismicity rate is a proxy of stress rate (Dieterich, 1994; Dieterich et al., 2000; Toda et al., 2002), the position of a PI hotspot is considered to reflect the area with significant temporal change in stress rate for change interval. In this study, we focused on the occurrence and non-occurrence of each large shallow earthquake in each prediction period following change interval with larger seismicity change than a threshold one; we changed the threshold in the statistical test using Molchan's diagram to check the robustness of the analysis result and to infer the characteristic time scale of precursory anomalous seismic activities. If PI hotspots are located on and/or near the epicenter of a large inland earthquake, it means that stress rate around the focal region of the earthquake becomes higher. Hence, the observation of temporal change in locations of PI hotspots is a key toward the physical understanding of stress state near the source area of a future large inland earthquake and its preparatory process. As described in Results section, our analysis identified PI hotspots on 8-to-10-yr time scales in regions on and/or near the focal regions of all target earthquakes prior to their occurrences.

Some previous studies examine such precursory seismicity changes of large inland earthquakes in Japan. Takahashi and Kumamoto (2006) discusses the relations of some seismic indices with the degree of fault evolution by investigating the temporal changes in the seismic indices prior to the occurrences of 8 large inland earthquakes in Japan, four of which are also focused on in this study (earthquake indices (C), (D), (E), and (G) in Table 1). The seismic indices include cumulative number of earthquakes, *a*-value and *b*-value of Gutenberg–Richter relation (Gutenberg and Richter, 1944), AS-function (Habermann, 1983), and LTA-function (Habermann, 1991; Wu and Chiao, 2006). They indicated that precursory seismic quiescence occurred on 1-to-7-yr time scales in 100-km-scale areas centered at the epicenters of large inland earthquakes (C), (D), (E), and (G) in Table 1. Apparently, the precursory time intervals on 1-to-7-yr time scales of abnormal seismic activities for earthquake indices (C), (D), (E), and (G) in Table 1 are inconsistent with those obtained in this study. This would be due to the differences of areas referred to in calculating the temporal changes in seismic activities; the areas of 204 km by 204 km and 312 km by 312 km used in this study are broader than those of 0.2° by 0.2° and 1.0° by 1.0° in Takahashi and Kumamoto (2006).

Yoshida and Aoki (2002) examined the seismic activities prior to the 1891 Nobi earthquake (Mikumo and Ando, 1976; Nakano et al., 2007), the 1964 Niigata earthquake (Hirasawa, 1965), the 1983 Central Japan Sea earthquake (Satake, 1985), and the 2000 Western Tottori Prefecture Earthquake in Japan (earthquake index (C) in Table 1) (Fukuyama et al., 2003; Ohmi et al., 2002). They indicated that the precursory seismic quiescence of the earthquakes occurred longer than 10 yr before the earthquakes. As to the 2000 Western Tottori Prefecture Earthquake, they showed that the precursory seismic quiescence began to occur 10 yr before its occurrence in a 150 by 350 km rectangular region including its source area. It should be noted that the earthquake occurrence probabilities obtained in this study are those for 204 by 204 km and 312 km-by-312 km square regions centered at respective calculation grids, which are almost the same scale as Yoshida and Aoki (2002). Hence, the precursory time interval on 8-to-10-yr time scales obtained in this study seems to be consistent with that obtained by Yoshida and Aoki (2002).

The PI method identifies the locations of anomalous seismic activities including both seismic quiescence and activation. This, therefore, corresponds to show the locations of stress relaxation and stress concentration in/around the source area of a future large earthquake. According to Yoshida and Aoki (2002), seismic quiescence occurred in a broader region around the source area of the 2000 Western Tottori Prefecture Earthquake, while seismicity remained active in the source area. Yoshida and Aoki (2002) interpreted the observation as due to the stress transfer into asperities on the source area that may be caused by a stress relaxation process in its surrounding region. Wyss et al. (1981) and Wyss (1986) also showed the same interpretation for the case of the 1975 Kalapana, Hawaii, earthquake and the 1983 Kaoiki, Hawaii, earthquake, respectively. On the other hand, by a numerical simulation using rate- and state-dependent friction laws (Ruina, 1983), Kato et al. (1997) demonstrated the appearance of regional seismic quiescence in the continental crust before a large interplate earthquake due to the regional stress relaxation could be caused by preseismic sliding on a boundary between a subducting oceanic plate and the overriding continental plate. Kato et al. (1997)

also argues that the mechanism of the seismic quiescence can also be applied to other types of earthquakes, such as intraplate earthquakes on active faults. Anomalous seismicity obtained in this study may thus reflect the temporal change in crustal seismicity associated with the regional stress relaxation prior to a large earthquake (Kawamura et al., 2013; Wu and Chiao, 2006; Wu et al., 2008).

We conclude that anomalous seismic activities of 8-to-10-yr time scales can precede the Japanese *M*6- or *M*7-class large shallow earthquakes. In considering the implications for the relation of this result to the preparatory process of large shallow earthquakes in Japan, it would be informative to investigate the existence of anomalous seismic activities preceding large earthquakes in other regions and, if any, their time scales to compare with the case for Japan. This may shed light on the comprehensive understanding of the occurrence mechanisms of large shallow earthquakes.

Acknowledgements. We thank the Japan Meteorological Agency (JMA) for the use of the unified earthquake catalog. Each hypocenter in the catalog is determined by analyzing in an integrated fashion the earthquake data of Hokkaido University, Hirosaki University, Tohoku University, the University of Tokyo, Nagoya University, Kyoto University, Kochi University, Kyushu University, Kagoshima University, National Research Institute for Earth Science and Disaster Prevention (NIED), National Institute of Advanced Industrial Science and Technology (AIST), Japan Agency for Marine-Earth Science and Technology (JAMSTEC), Tokyo Metropolitan Government, Yokohama City, Shizuoka Prefecture, Hot Springs Research Institute of Kanagawa Prefecture, and JMA. Data can be obtained from the Japan Meteorological Business Support Center. This research was financially supported by the National Science Council (R.O.C.).

References

Arabasz, W. J. and Wyss, M.: Significant precursory seismic quiescences in the extensional Wasatch Front region, Utah, EOS Trans. AGU, vol. 77, p. F455, 1996.

Borovik, N., Misharina, L., and Treskov, A.: On the possibility of strong earthquakes in Pribakalia in the future, Izv.-Phys. Solid Eart.+, 1, 13–16, 1971 (English translation).

Bowman, D. D. and King, G. C. P.: Accelerating seismicity and stress accumulation before large earthquakes, Geophys. Res. Lett., 28, 4039–4042, 2001.

Bowman, D. D., Ouillon, G., Sammis, G., Sornette, A., and Sornette, D.: An observed test of the critical earthquake concept, J. Geophys. Res., 103, 24359–24372, 1998.

Bufe, C. G. and Varnes, D. J.: Predictive modeling of the seismic cycle of the greater San Francisco Bay region, J. Geophys. Res., 98, 9871–9883, 1993.

Bufe, C. G., Nishenko, S. P., and Varnes, D. J.: Seismicity trends and potential for large earthquakes in the Alaska–Aleutian region, Pure Appl. Geophys., 142, 83–99, 1994.

Chen, C. C.: Accelerating seismicity of moderate-size earthquakes before the 1999 Chi-Chi, Taiwan, earthquake: testing time-prediction of the self-organizing spinodal model of earthquakes, Geophys. J. Int., 155, F1–F5, 2003.

Chen, C. C. and Wu, Y. X.: An improved region-time-length algorithm applied to the 1999 Chi-Chi, Taiwan earthquake, Geophys. J. Int., 166, 1144–1147, 2006.

Chen, C. C., Rundle, J. B., Holliday, J. R., Nanjo, K. Z., Turcotte, D. L., Li, S. C., and Tiampo, K. F.: The 1999 Chi-Chi, Taiwan, earthquake as a typical example of seismic activation and quiescence, Geophys. Res. Lett., 32, L22315, doi:10.1029/2005GL023991, 2005.

Chen, C. C., Rundle, J. B., Li, H. C., Holliday, J. R., Nanjo, K. Z., Turcotte, D. L., and Tiampo, K. F.: From tornadoes to earthquakes: forecast verification for binary events applied to the 1999 Chi-Chi, Taiwan, earthquake, Terr. Atmos. Ocean. Sci., 17, 503–516, 2006.

Console, R., Montuori, C., and Murru, M.: Statistical assessment of seismicity patterns in Italy: are they precursors of subsequent events?, J. Seismol., 4, 435–449, 2000.

Dieterich, J.: A constitutive law for rate of earthquake production and its application to earthquake clustering, J. Geophys. Res., 99, B2, doi:10.1029/93JB02581, 1994.

Dieterich, J., Cayol, V., and Okubo, P.: The use of earthquake rate changes as a stress meter at Kilauea volcano, Nature, 408, 457–460, 2000.

Gutenberg, B. and Richter, D. F.: Frequency of earthquakes in California, B. Seismol. Soc. Am., 34, 185–188, 1944.

Habermann, R. E.: Teleseismic detection in the Aleutian island arc, J. Geophys. Res., 88, 5056–5064, 1983.

Habermann, R. E.: Man-made changes of seismicity rates, B. Seismol. Soc. Am., 77, 141–159, 1987.

Habermann, R. E.: Seismicity rate variations and systematic changes in magnitudes in teleseismic catalogs, Tectonophysics, 193, 277–289, 1991.

Hirasawa, T.: Source mechanism of the Niigata Earthquake of June 16, 1964, as derived from body waves, J. Phys. Earth, 13, 35–66, 1965.

Holliday, J. R., Nanjo, K. Z., Tiampo, K. F., Rundle, J. B., Turcotte, D. L., and Donnellan, A.: Forecasting the locations of future earthquake and its verification, Nonlinear Proc. Geoph., 12, 965–977, 2005.

Holliday, J. R., Rundle, J. B., Tiampo, K. F., Klein, W., and Donnellan, A.: Systematic procedural and sensitivity analysis of the pattern informatics method for forecasting large ($M > 5$) earthquake events in southern California, Pure Appl. Geophys., 163, 2433–2454, 2006.

Huang, Q., Sobolev, G. A., and Nagao, T.: Characteristics of the seismic quiescence and activation patterns before the $M = 7.2$ Kobe earthquake, January 17, 1995, Tectonophysics, 337, 99–116, 2001.

Imanishi, K., Kuwahara, Y., and Haryu, Y.: Off-fault aftershocks of the 2005 West Off Fukuoka Prefecture Earthquake: reactivation of a structural boundary?, Earth Planets Space, 58, 81–86, 2006.

Jaume, S. C. and Sykes, L. R.: Evolving towards a circular point: a review of accelerating seismic moment/energy release prior to large and great earthquakes, Pure Appl. Geophys., 155, 279–306, 1999.

Kagan, Y. Y.: On earthquake predictability measurement: information score and error diagram, Pure Appl. Geophys., 164, 1947–1962, 2007.

Karakaisis, G. F., Papazachos, C. B., Savvaidis, A. S., and Papazachos, B. C.: Accelerating seismic crustal deformation in the North Aegean Trough, Greece, Geophys. J. Int., 148, 193–200, 2002.

Kato, N., Ohtake, M., and Hirasawa, T.: Possible mechanism of precursory seismic quiescence: regional stress relaxation due to preseismic sliding, Pure Appl. Geophys., 150, 249–267, 1997.

Katsumata, K.: A long-term seismic quiescence started 23 years before the 2011 off the Pacific coast of Tohoku Earthquake ($M = 9.0$), Earth Planets Space, 63, 709–712, 2011a.

Katsumata, K.: Precursory seismic quiescence before the $M_w = 8.3$ Tokachi-oki, Japan, earthquake on 26 September 2003 revealed by a re-examined earthquake catalog, J. Geophys. Res., 116, B10307, doi:10.1029/2010JB007964, 2011b.

Kawamura, M., Wu, Y. H., Kudo, T., and Chen, C. C.: Precursory migration of anomalous seismic activity revealed by the pattern informatics method: a case study of the 2011 Tohoku earthquake, Japan, B. Seismol. Soc. Am., in press, 2013.

Kisslinger, K. and Kindel, B.: A comparison of seismicity rates near Adak island, Alaska, September 1988 through May 1990 with rates before the 1982 to 1986 apparent quiescence, B. Seismol. Soc. Am., 84, 1560–1570, 1994.

Ma, K.-F., Chan, C.-H., and Stein, R. S.: Response of seismicity to Coulomb stress triggers and shadows of the 1999 $M_\mathrm{w} = 7.6$ Chi-Chi, Taiwan, earthquake, J. Geophys. Res., 110, B05S19, doi:10.1029/2004JB003389, 2005.

Mikumo, T. and Ando, M.: A search into the faulting mechanism of the 1891 great Nobi earthquake, J. Phys. Earth., 24, 63–87, 1976.

Mogi, K.: Some features of recent seismic activity in and near Japan (2), B. Earthq. Res. I. Tokyo, 46, 30–36, 1969.

Mogi, K.: Earthquake Prediction, Academic Press Japan, 1985.

Murru, M., Console, R., and Montuori, C.: Seismic quiescence precursor to the 1983 Nihonkai-Chubu ($M7.7$) earthquake, Japan, Ann. Geofis., 42, 871–882, 1999.

Nagao, T., Takeuchi, A., and Nakamura, K.: A new algorithm for the detection of seismic quiescence: introduction of the RTM algorithm, a modified RTL algorithm, Earth Planets Space, 63, 315–324, 2011.

Nakano, M., Miyakoshi, J., and Yamaoka, K.: A new model for the fault beneath the sedimentary basin in the 1891 Nobi earthquake, Earth Planets Space, 59, 13–19, 2007.

Ogata, Y.: Seismicity quiescence and activation in western Japan associated with the 1944 and 1946 great earthquakes near the Nankai trough, J. Geophys. Res., 109, B04305, doi:10.1029/2003JB002634, 2004.

Ogata, Y.: Detection of anomalous seismicity as a stress change sensor, J. Geophys. Res., 110, B05S06, doi:10.1029/2004JB003245, 2005.

Öztürk, S. and Bayrak, Y.: Spatial variations of precursory seismic quiescence observed in recent years in the eastern part of Turkey, Acta Geophys., 60, 92–118, 2012.

Papazachos, B. C., Karakaisis, G. F., Scordilis, E. M., Papazachos, C. B., and Panagiotopoulos, D. G.: Present patterns of decelerating-accelerating seismic strain in South Japan, J. Seismol., 14, 273–288, doi:10.1007/s10950-009-9165-z, 2010.

Papazachos, C. B., Karakaisis, G. F., Scordilis, E. M., and Papazachos, B. C.: Global observational properties of the critical earthquake model, B. Seismol. Soc. Am., 95, 1841–1855, 2005.

Resenberg, P. A. and Matthews, M. V.: Precursory seismic quiescence: a preliminary assessment of the hypothesis, Pure Appl. Geophys., 126, 373–406, 1988.

Title Page
Abstract Introduction
Conclusions References
Tables Figures
I◀ ▶I
◀ ▶
Back Close
Full Screen / Esc
Printer-friendly Version
Interactive Discussion

Ruina, A. L.: Slip instability and state variable friction laws, J. Geophys. Res., 88, 10359–10370, 1983.

Rundle, J. B., Klein, W., Tiampo, K., and Gross, S.: Linear pattern dynamics in nonlinear threshold systems, Phys. Rev. E, 61, 2418–2431, 2000.

Rundle, J. B., Tiampo, K. F., Klein, W., and Martins, J. S. Sá: Self-organization in leaky threshold systems: the influence of near-mean field dynamics and its implications for earthquakes, neurobiology, and forecasting, P. Natl. Acad. Sci. USA, 99, 2514–2521, 2002.

Rundle, J. B., Turcotte, D. L., Shcherbakov, R., Klein, W., and Sammis, C.: Statistical physics approach to understanding the multiscale dynamics of earthquake fault systems, Rev. Geophys., 41, 1019, doi:10.1029/2003RG000135, 2003.

Satake, K.: The mechanism of the 1983 Japan Sea earthquake as inferred from long-period surface waves and tsunamis, Phys. Earth Planet. In., 37, 249–260, 1985.

Shcherbakov, R., Turcotte, D. L., Rundle, J. B., Tiampo, K. F., and Holliday, J. R.: Forecasting the locations of future large earthquakes: an analysis and verification, Pure Appl. Geophys., 167, 743–749, 2010.

Sobolev, G. A.: Application of the RTL algorithm to the analysis of preseismic processes before strong earthquakes in California, Äul Izv.-Phys. Solid Eart.+, 39, 179–188, 2003.

Stein, R. S.: The role of stress transfer in earthquake occurrence, Nature, 402, 605–609, 1999.

Stuart, W. D.: Seismic quiescence at Parkfield due to detachment faulting, Nature, 349, 58–61, 1991.

Sykes, L. R. and Jaume, S. C.: Seismic activity on neighboring faults as a long-term precursor to large earthquakes in the San Francisco Bay area, Nature, 348, 595–599, 1990.

Takahashi, N. and Kumamoto, T.: Preliminary investigation of seismicity rate change immediately before mainshock and fault maturity for damaging intraplate earthquakes in Japan, Active Fault Research, 26, 15–28, 2006 (in Japanese with English abstract).

Tiampo, K. F., Rundle, J. B., McGinnis, S., Gross, S. J., and Klein, W.: Mean-field threshold systems and phase dynamics: an application to earthquake fault systems, Europhys. Lett., 60, 481–487, 2002.

Toda, S., Stein, R. S., and Sagiya, T.: Evidence from the AD 2000 Izu islands earthquake swarm that stressing rate governs seismicity, Nature, 419, 58–61, 2002.

Wei, G., Lin, Z., Zhu, X., Zhao, Y., Zhao, X., and Hou, H.: On seismic gaps previous to certain great earthquakes occurred in north China, Acta Geophys. Sinica, 21, 213–217, 1978.

Wu, Y. H., Chen, C. C., and Rundle, J. B.: Precursory seismic activation of the Pintung (Taiwan) offshore doublet earthquakes on 26 December 2006: a pattern informatics analysis, Terr. Atmos. Ocean. Sci., 19, 743–749, 2008a.

Wu, Y. H., Chen, C. C., and Rundle, J. B.: Detecting precursory earthquake migration patterns using the pattern informatics method, Geophys. Res. Lett., 35, L19304, doi:10.1029/2008GL035215, 2008b.

Wu, Y. H., Chen, C. C., and Rundle, J. B.: Precursory small earthquake migration patterns, Terra Nova, 23, 369–374, 2011.

Wu, Y. M. and Chen, C. C. Seismic reversal pattern for the 1999 Chi-Chi, Taiwan, M_w7.6 earthquake, Tectonophysics, 429, 125–132, 2007.

Wu, Y. M. and Chiao, L. Y.: Seismic quiescence before the 1999 Chi-Chi, Taiwan, M_w7.6 earthquake, B. Seismol. Soc. Am., 96, 321–327, 2006.

Wyss, M.: Seismic quiescence precursor to the 1983 Kaoiki ($M_s = 6.6$), Hawaii, Earthquake, B. Seismol. Soc. Am., 76, 785–800, 1986.

Wyss, M. and Wiemer, S.: Two current seismic quiescences within 40 km of Tokyo, Geophys. J. Int., 128, 459–473, 1997.

Wyss, M. and Wiemer, S.: How can one test the seismic gap hypothesis? The Case of repeated ruptures in the Aleutians, Pure Appl. Geophys., 155, 259–278, 1999.

Wyss, M., Klein, F. W., and Johnston, A. C.: Precursors to the Kalapana $M = 7.2$ Earthquake, J. Geophys. Res., 86, 3881–3900, 1981.

Yoshida, A. and Aoki, G.: Seismic quiescence in a large area along the coast of the Japan Sea before large earthquakes, J. Geogr., 111, 212–221, 2002 (in Japanese with English abstract and Figure captions).

Yu, H. Z., Cheng, J., Zhang, X. T., Zhang, L. P., Liu, J., and Zhang, Y. X.: Multi-methods combined analysis of future earthquake potential, Pure Appl. Geophys., 170, 173–183, 2013.

Zheng, B., Hamburger, M. W., and Popandopulo, G. A.: Precursory seismicity changes preceeding moderate and large earthquakes in the Garm region, Central Asia, B. Seismol. Soc. Am., 85, 571–589, 1995.

Table 1. Earthquake index assigned to each of 12 large earthquakes with magnitudes larger than $M = 6.4$ and the corresponding occurrence date, epicenter (longitude and latitude), depth, and magnitude.

Earthquake index	Date	Longitude (degree)	Latitude (°)	Depth (km)	Magnitude
(A)	1 Jul 2000	139.19	34.19	16.1	6.5
(B)	30 Jul 2000	139.41	33.97	17.0	6.5
(C)	6 Oct 2000	133.35	35.27	9.0	7.3
(D)	26 Jul 2003	141.17	38.41	11.9	6.4
(E)	23 Oct 2004	138.87	37.29	13.1	6.8
(F)	23 Oct 2004	138.93	37.31	14.2	6.5
(G)	20 Mar 2005	130.18	33.74	9.2	7.0
(H)	25 Mar 2007	136.69	37.22	10.7	6.9
(I)	16 Jul 2007	138.61	37.56	16.8	6.8
(J)	14 Jun 2008	140.88	39.03	7.8	7.2
(K)	20 Dec 2008	142.70	36.53	0.0	6.6
(L)	11 Aug 2009	138.50	34.79	23.3	6.5

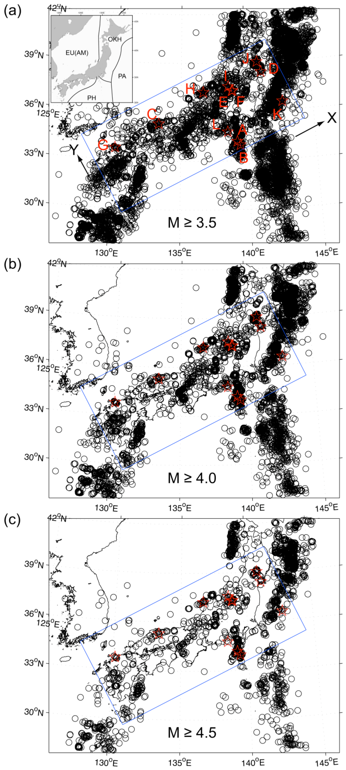

Fig. 1. Maps showing epicenters within rectangular regions used for PI analysis for threshold magnitudes of **(a)** 3.5, **(b)** 4.0, and **(c)** 4.5, respectively. Labels (A) to (L) correspond to earthquake indices in Table 1. With regard to x- and y-axes of the rectangular region, refer to Fig. 2b. The inset of panel **(a)** shows a map view of the tectonic setting around the Japanese islands; PA: Pacific plate, PH: Philippine Sea plate, EU (AM): Eurasian plate (Amurian plate), OKH: Okhotsk plate.

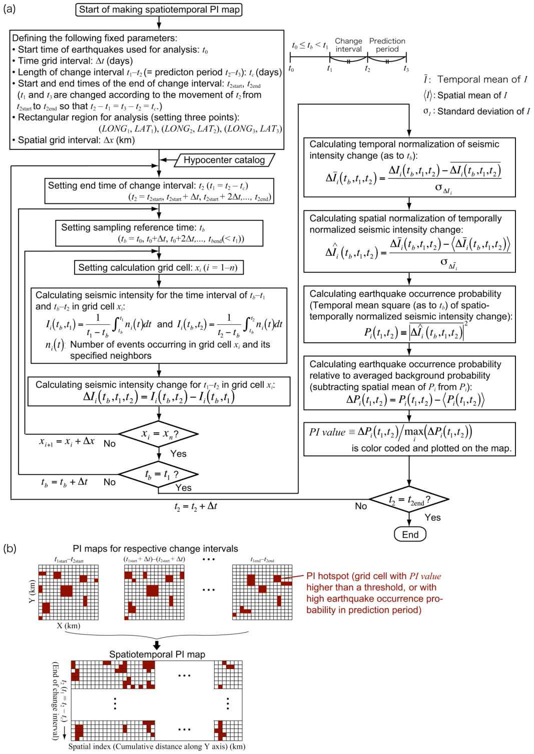

Fig. 2. **(a)** Flowchart of the procedure for obtaining PI maps, which denote the spatial distribution of grid cells with earthquake occurrence probabilities higher than a particular threshold (PI hotspots). **(b)** Illustration of the method for obtaining the spatiotemporal PI map obtained by combining PI maps obtained based on the process shown in panel **(a)**. x- and y-axes correspond to those in Fig. 1.

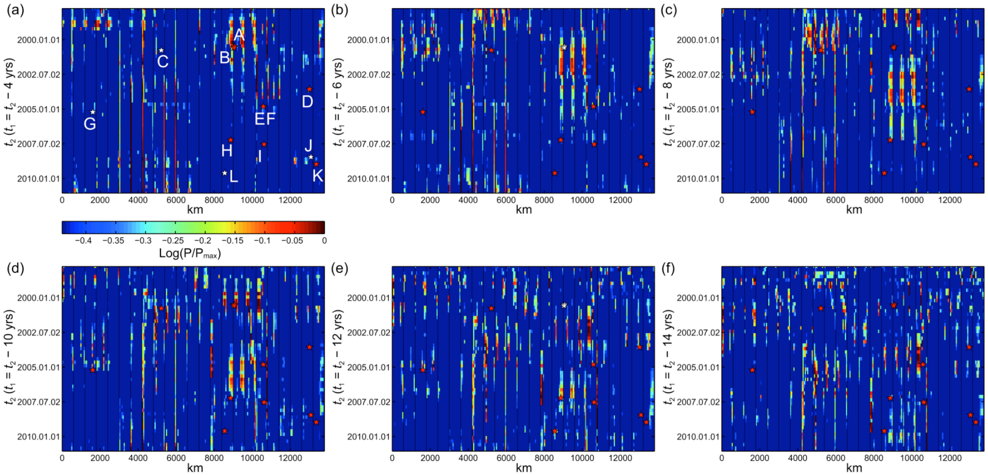

Fig. 3. Spatiotemporal PI maps for a cut-off magnitude of 3.5, which denote the locations of grid cells with large seismicity changes (PI hotspots) for different change intervals between t_1 and t_2 ($t_2 - t_1$ = 4, 6, 8, 10, 12, and 14 yr, t_2 = 1 January 1997–28 February 2011). Length of change interval for each panel is shown after "t_1−" in parenthesis of the label of vertical axis. Grid cells with earthquake occurrence probabilities higher than −0.4 are regarded as locations with large seismicity changes, including seismic quiescence and activation, during change interval. Red-color grid cells correspond to the highest probability of earthquake occurrence. Deep blue ones lower than −0.4 represent locations with small seismicity changes, indicating low probabilities of earthquake occurrences in prediction periods following change intervals. Refer to Fig. 2b on horizontal and vertical axes. Each vertical black line denotes the end of y-axis (refer to Figs. 1 and 2b). Labels (A) to (L) correspond to earthquake indices in Table 1.

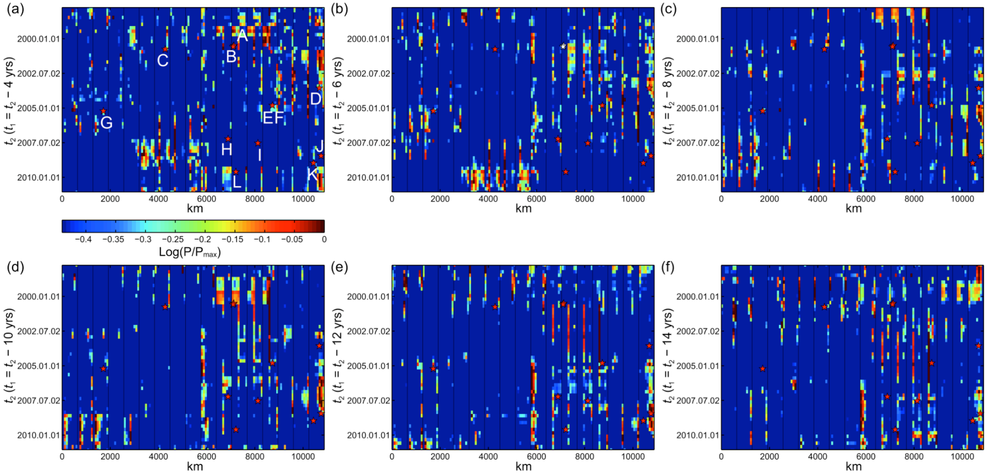

Fig. 4. The same maps as shown in Fig. 3 but for a cut-off magnitude of 4.0.

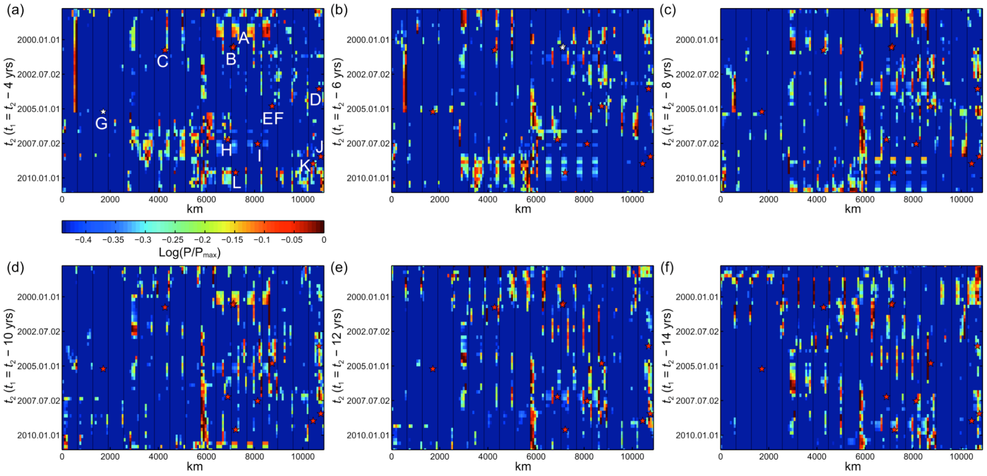

Fig. 5. The same maps as shown in Fig. 3 but for a cut-off magnitude of 4.5.

Title Page
Abstract | Introduction
Conclusions | References
Tables | Figures
◀| |▶
◀ ▶
Back | Close
Full Screen / Esc
Printer-friendly Version
Interactive Discussion

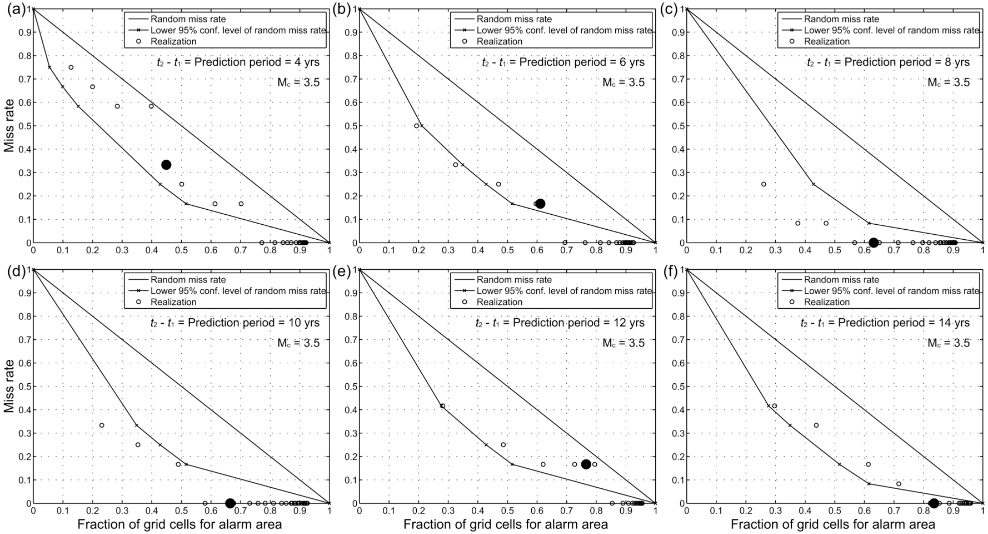

Fig. 6. Molchan's error diagrams for different change intervals between t_1 and t_2 ($t_2 - t_1 = 4$, 6, 8, 10, 12, and 14 yr, t_2 = 1 January 1997–28 February 2011). Vertical axis denotes miss rate, which is defined as the number of $M \geqq 6.4$ events that occurred outside alarm area relative to their total. Horizontal axis shows fraction of union of grid cells occupied by prediction periods following change intervals with earthquake occurrence probabilities higher than −0.4.

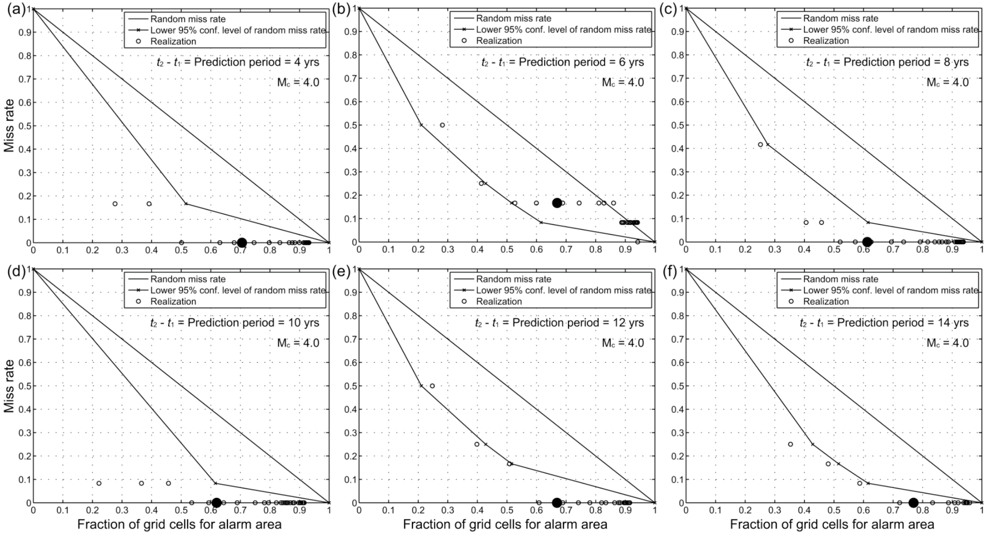

Fig. 7. The same diagrams as shown in Fig. 6 but for a cut-off magnitude of 4.0.

Title Page
Abstract | Introduction
Conclusions | References
Tables | Figures
◀I | ▶I
◀ | ▶
Back | Close
Full Screen / Esc
Printer-friendly Version
Interactive Discussion

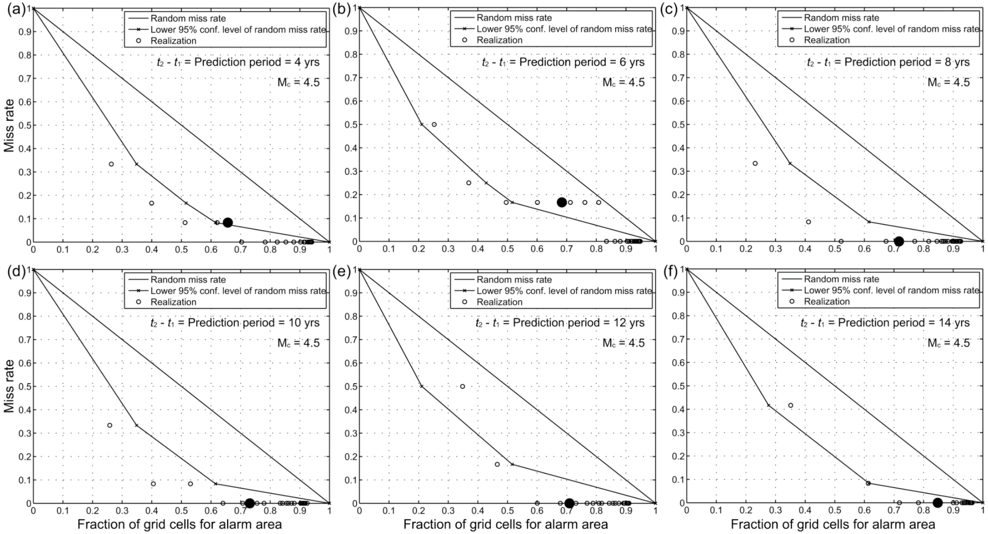

Fig. 8. The same diagrams as shown in Fig. 6 but for a cut-off magnitude of 4.5.